

Microcontact printing with aminosilanes: creating biomolecule micro- and nanoarrays for multiplexed microfluidic bioassays

Shivani Sathish,[‡] Sébastien G. Ricoult,[‡] Kazumi Toda-Peters and Amy Q. Shen*

Micro/Bio/Nanofluidics Unit, Okinawa Institute of Science and Technology Graduate University,
Okinawa, 904-0495 Japan

1. Schematics of stamps for microcontact printing and microfluidic devices

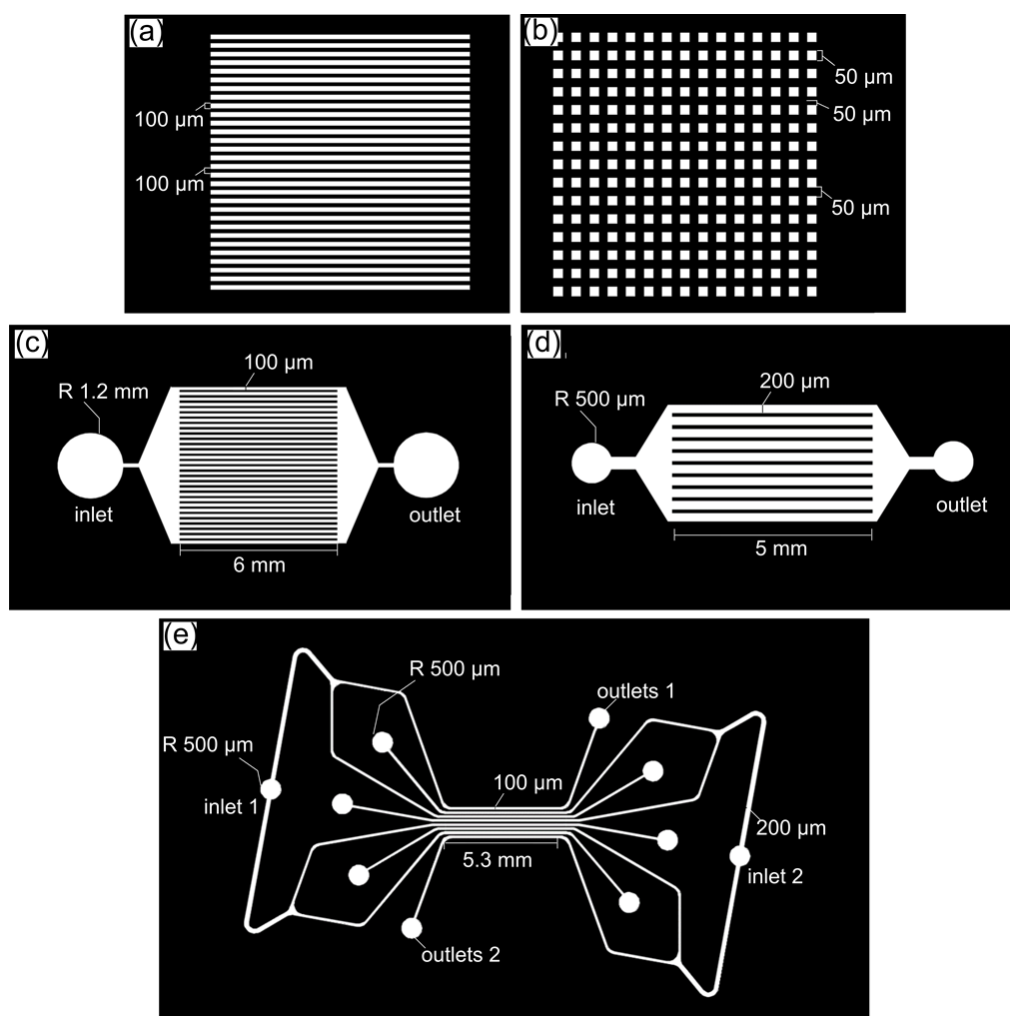


Fig S1: Patterning stamp designs by AutoCAD (AutoDesk, USA) drawings: (a) 100 μm wide stripes with 100 μm spacing; (b) an array of 50 by 50 μm squares with 50 μm spacing. Microfluidic device designs by AutoCAD: (c) 100 μm wide and (d) 200 μm wide parallel channels with single inlet and single outlet, for unidirectional flows; and (e) 200 μm wide parallel channels connected with two different inlets, for opposite flow directions in alternating channels.

2. Comparing the effect of flow on physisorbed vs covalently patterned biomolecules in microfluidic channels

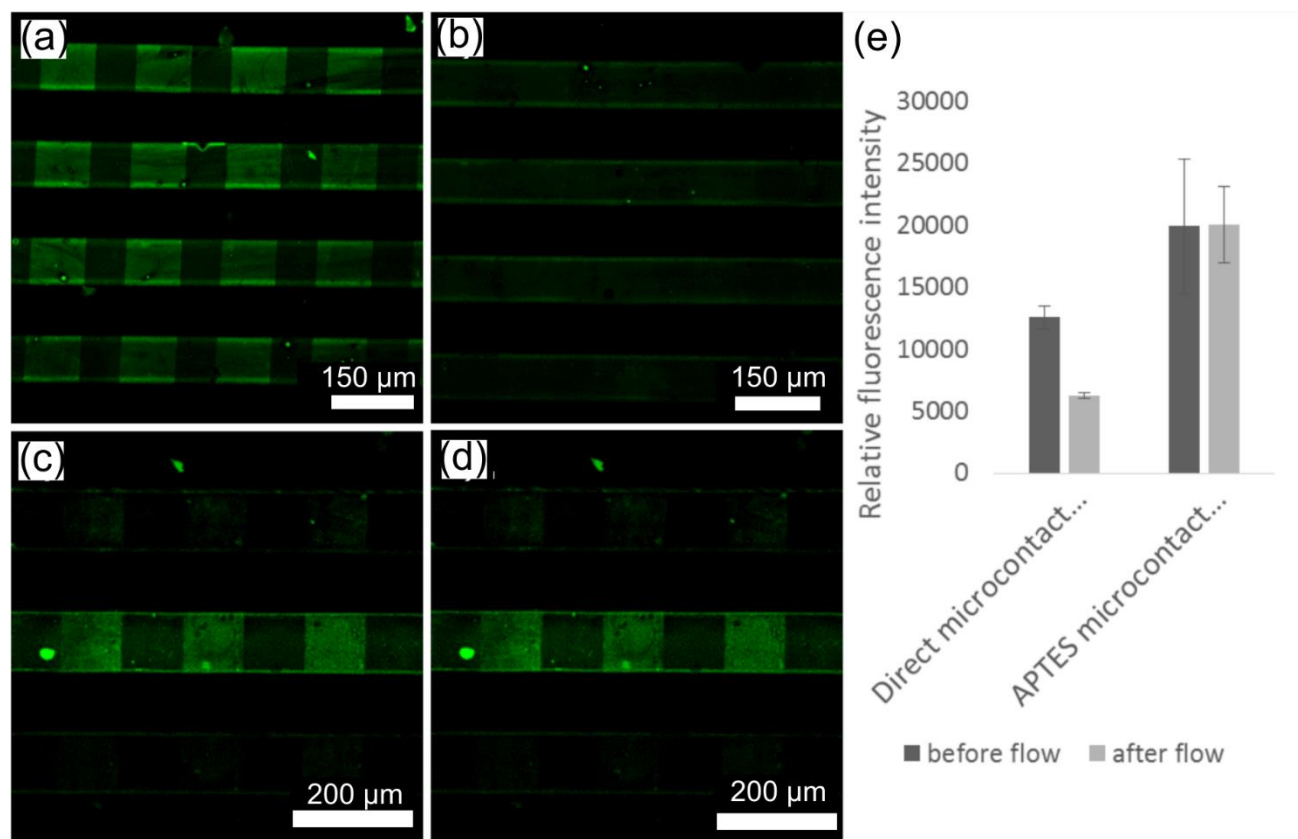


Fig S2: Covalent patterning of biomolecules on surfaces using covalent microcontact printing. Conventional microcontact printing of fluorescently-labeled IgG (shown in green) in microfluidic channels yields (a) microarrays prior to flow, (b) fluorescence in the regions of protein deposition diminishes due to flow in the microfluidic device and protein detachment. Covalent grafting of the proteins using covalent microcontact printing yields (c) microarrays prior to flow, (d) fluorescence intensity remain the same under high flow rates and proteins remain bound to the surface. (e) Quantification of the fluorescence intensity verifies that protein remains bound to the surface under flow conditions via the covalent grafting approach.

3. Nanocontact printing of proteins vs grafting biomolecules onto nanocontact printed APTES

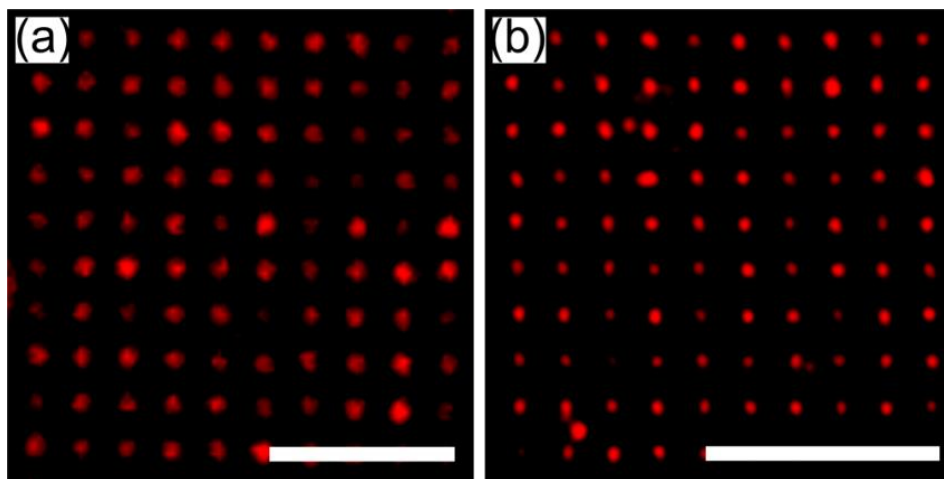


Fig S3: Comparison of direct protein nanocontact printing and aqueous-based APTES nanocontact printing. (a) Conventional nanocontact printing was performed to directly pattern a glass substrate with nanoarrays of fluorescently labelled Immunoglobulins (IgGs) (red) of 200 nm feature size, using the procedure previously described by Ricoult et al., (2013) [1]. The nanopatterns of fluorescently labeled protein were imaged on an LSM 780 Confocal microscope (Zeiss, Japan). (b) A plasma-activated NOA63 lift-off stamp was contacted with an APTES_{aq}-inked PDMS flat stamp. The APTES_{aq} patterned flat stamp was pressed onto a plasma activated glass slide for 5 s. A microfluidic channel was then bonded irreversibly to encapsulate the nanoarrays. Fluorescence images reveal fluorescently-labeled IgGs grafted onto the APTES_{aq} nanoarrays of 200 nm feature size within the microfluidic channels. These images demonstrate that the biomolecular nanoarrays generated via nanocontact printing of APTES_{aq} followed by IgG grafting is similar to the nanoarrays created by direct nanocontact printing of IgGs. Scale bars are 6 μm in both (a) & (b).

4. Antibody-based sandwich immunoassay for detection of human C-reactive protein (hCRP)

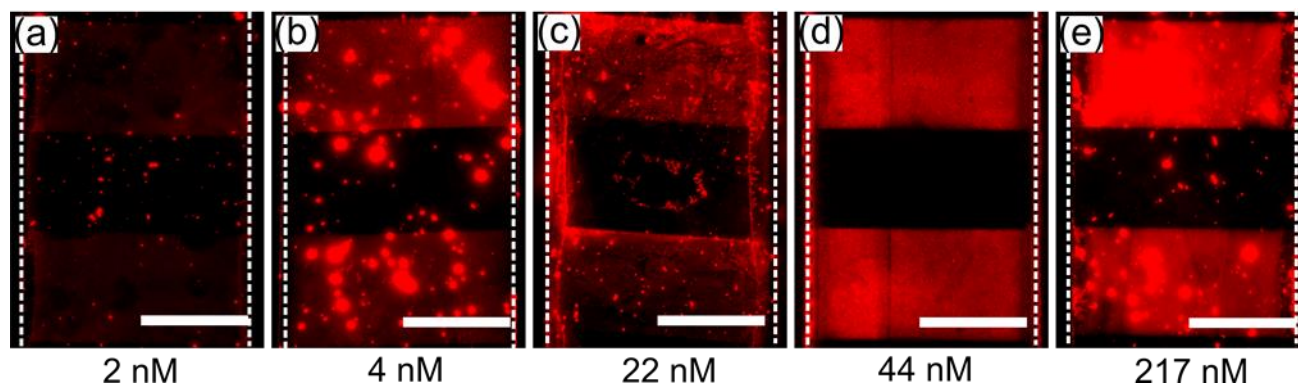


Fig S4: Antibody-based sandwich immunoassay to detect human C-reactive protein (hCRP).

Microchannel (microfluidic channel boundaries shown in white dotted lines) substrates are first patterned with APTES_{aq} patterns with capture antibodies grafted via BS3 chemistry. hCRP with concentrations varying from 2 nM to 217 nM are mixed with 1 × PBS and flowed through the microfluidic device. Captured hCRP molecules were detected via a secondary antibody pair consisting of the same primary antibody and Alexa-fluor 546-labelled fluorescent secondary antibody. Red squares in the images depict positive capture and detection of hCRP at varying concentrations, with fluorescence intensities proportional to the concentration of hCRP. Black squares depict unpatterned and blocked regions which serve as background. Scale bars are 200 μm.

Reference

1. Ricoult, S.G., et al., *Large Dynamic Range Digital Nanodot Gradients of Biomolecules Made by Low-Cost Nanocontact Printing for Cell Haptotaxis*. *Small*, 2013. **9**(19): p. 3308-3313.